Available online at www.sciencedirect.com
ScienceDirect
Journal of Power Sources 168 (2007) 546–552
JOURNAL OF POWER SOURCES
www.elsevier.com/locate/jpowsour

Carbon nanofibre/hydrous RuO_2 nanocomposite electrodes for supercapacitors

Byung Jun Lee [a], S.R. Sivakkumar [a], Jang Myoun Ko [a,*], Jong Huy Kim [b], Seong Mu Jo [c], Dong Young Kim [d]

[a] *Department of Applied Chemistry & Biotechnology, Hanbat National University, San 16-1, Dukmyung-Dong, Yusung-Gu, Daejeon 305-719, South Korea*
[b] *Energy Storage Research Center in Korea Institute of Energy Research, 71-2, Jang-dong, Yusung-Gu, Daejeon 305-343, Republic of Korea*
[c] *Polymer Hybrid Research Center, Korea Institute of Science and Technology, P.O. Box 131, Cheongryang, Seoul 130-650, South Korea*
[d] *Optoelectronic Materials Research Center, Korea Institute of Science and Technology, P.O. Box 131, Cheongryang, Seoul 130-650, South Korea*

Received 5 December 2006; accepted 18 February 2007
Available online 12 March 2007

Abstract

Amorphous $RuO_2{\cdot}xH_2O$ and a VGCF/$RuO_2{\cdot}xH_2O$ nanocomposite (VGCF = vapour-grown carbon fibre) are prepared by thermal decomposition. The morphology of the materials is investigated by means of scanning electron microscopy. The electrochemical characteristics of the materials, such as specific capacitance and rate capability, are investigated by cyclic voltammetry over a voltage range of 0–1.0 V at various scan rates and with an electrolyte solution of 1.0 M H_2SO_4. The specific capacitance of $RuO_2{\cdot}xH_2O$ and VGCF/$RuO_2{\cdot}xH_2O$ nanocomposite electrodes at a scan rate of 10 mV s^{-1} is 410 and 1017 F g^{-1}, respectively, and at 1000 mV s^{-1} are 258 and 824 F g^{-1}, respectively. Measurements of ac impedance spectra are made on both the electrodes at various bias potentials to obtain a more detailed understanding of their electrochemical behaviour. Long-term cycle-life tests for 10^4 cycles shows that the $RuO_2{\cdot}xH_2O$ and VGCF/$RuO_2{\cdot}xH_2O$ electrodes retain 90 and 97% capacity, respectively. These encouraging results warrant further development of these electrode materials towards practical application.

Keywords: Supercapacitor; Hydrous ruthenium oxide; Vapour-grown carbon fibre; Electrochemical capacitor; Capacity retention; Morphology

1. Introduction

Supercapacitors are highly attractive energy-storage devices due to their exceptionally high power and energy density characteristics compared with conventional dielectric capacitors, and to their long cycle-life with respect to batteries. Hence, these supercapacitors are finding important applications in electric and hybrid electric vehicles, camera flash equipment, pulse light generators, power back-up in electronic devices, etc. [1]. There are two types of supercapacitor, namely: (i) carbon-based electric double-layer supercapacitors (EDLCs) and (ii) conducting polymer or metal oxide-based electrochemical supercapacitors.

In terms of long cycle-life and high specific capacitance, carbon and transition metal oxides have been recognized as promising electrode materials for supercapacitors. Activated carbons [2–7], carbon nanotubes (CNTs) [8], carbon fibres [9–11] and carbon aerogels [12,13] are some of the materials that have been investigated for their charge-storage behaviour. Among them, activated carbon is the cheapest material and hence many research activities have been devoted to its development as a supercapacitor electrode. Despite the high specific capacitance (up to 250 F g^{-1}) of carbonaceous materials, they suffer from poor specific energy density. Metal oxides such as RuO_2 [14–22], MnO_2 [23,24], NiO_x [25,26], IrO_2 [27], etc. are also under evaluation for their charge-storage behaviour. Among all of these metal oxides, RuO_2 in its amorphous hydrous form ($RuO_2{\cdot}xH_2O$) has been found to be the best material for supercapacitor applications due to its high specific capacitance, high specific energy density, high electrochemical reversibility, and long cycle-life. Nevertheless, an intrinsic problem with $RuO_2{\cdot}xH_2O$ is that only a very thin layer takes part in the charge-storage mechanism while the underlying active material remains unreacted. Further, $RuO_2{\cdot}xH_2O$ suffers from poor high-rate capability and is also expensive.

* Corresponding author. Tel.: +82 42 821 1545; fax: +82 42 821 1593.
E-mail address: jmko@hanbat.ac.kr (J.M. Ko).

0378-7753/$ – see front matter © 2007 Elsevier B.V. All rights reserved.
doi:10.1016/j.jpowsour.2007.02.076

Therefore, many of studies have been made by hybridizing high surface-area ($\sim$2000 $m^2\,g^{-1}$) carbon materials with $RuO_2{\cdot}xH_2O$ as a composite for supercapacitor applications to exploit the advantages of these two individual components [28–46]. Depending upon the loading and thickness of the $RuO_2{\cdot}xH_2O$ in carbon matrices, a wide range of specific capacitances from 150 $F\,g^{-1}$ (for thick film) to 1540 $F\,g^{-1}$ (for thin film) has been reported for these composite materials. In most of these composites, a high loading of $RuO_2{\cdot}xH_2O$ on the carbon matrix, say, more than $\sim$40 wt.% is observed to decrease the specific capacitance and rate capability of the composite electrodes due to the thickness issue of $RuO_2{\cdot}xH_2O$ [31,32,39,43,46]. On the other hand, in order to realize higher specific energy density from the composite electrode, an increased loading of $RuO_2{\cdot}xH_2O$ is necessary. Hence, the drawbacks pertaining to both the individual components of activated carbon and $RuO_2{\cdot}xH_2O$ have only been partially solved in the composite materials. It should also be noted that, when $RuO_2{\cdot}xH_2O$ is loaded heavily (say, >50 wt.%) on the high surface-area ($\sim$2000 $m^2\,g^{-1}$) carbon, whose intrinsic specific capacitance may be as high as 250 $F\,g^{-1}$, all the surface of the carbon will be coated with the $RuO_2{\cdot}xH_2O$. As a consequence, the double-layer capacitance of the active carbon will become negligible due to the blockage of the carbon surface and hence the total specific capacitance of the composite material will be governed mainly by the Faradaic pseudocapacitance of the $RuO_2{\cdot}xH_2O$ material. When the composite is partially loaded (say, <30 wt.%) with $RuO_2{\cdot}xH_2O$, however, both the double-layer capacitance of the active carbon and the pseudo capacitance arising from the Faradaic reactions of $RuO_2{\cdot}xH_2O$ will contribute concomitantly to the charge-storage process. Quantifying the individual contribution of these two processes to the total specific capacitance is often difficult. In some instances, therefore, it is hard to realize whether the loading of $RuO_2{\cdot}xH_2O$ on high surface-area carbon has caused any improvement in the specific capacitance of the composite material or not. On the other hand, when a carbon material having a very low specific capacitance is used as a matrix, the effect of its hybridization with $RuO_2{\cdot}xH_2O$ can be understood more clearly.

To this end, in the present study, a relatively cheap carbon material, namely, vapour-grown carbon fibre (VGCF), with a specific capacitance as low as 1.9 $F\,g^{-1}$, is chosen as a matrix for the dispersion of $RuO_2{\cdot}xH_2O$. Because of the very low specific capacitance of the VGCF, the effect of $RuO_2{\cdot}xH_2O$ loading over its surface can be realized without ambiguity. Most importantly, VGCF is a substantially more conductive (specific resistance: 0.012 Ω cm) carbon material than conventional activated carbons (specific resistance range: 0.04–1.0 Ω cm). This feature is believed to play a favourable role as a matrix material for even a relatively high surface loading of $RuO_2{\cdot}xH_2O$ so that this composite is expected to display better high-rate performance, which is often difficult to achieve in activated carbon-based composites. To the best of our knowledge, until now there has not been any report of the use of VGCF/$RuO_2{\cdot}xH_2O$ nanocomposite material for charge-storage applications. Thus, it would appear that the electrochemical characteristics of this nanocomposite (and for comparative purpose those of, pristine $RuO_2{\cdot}xH_2O$) as an electrode material for supercapacitors are presented for the first time.

2. Experimental

The VGCF (Showa Denko K.K, Japan) used in this study had the specific surface-area of 13 $m^2\,g^{-1}$, a specific resistance of 0.012 Ω cm, and an aspect ratio of 67. All other chemicals were purchased from Aldrich and used as received. Triple-distilled water of 18 MΩ obtained from aqua MAX water system (Younglin, Korea) was used to prepare the solutions. Platinum electrodes were cleaned with Piranha solution.

Synthesis of pristine $RuO_2{\cdot}xH_2O$ and the VGCF/$RuO_2{\cdot}xH_2O$ nanocomposite was carried out by following a procedure similar to that reported in an earlier publication [35], which is briefly described as follows. A stoichiometric quantity of $RuO_2{\cdot}xH_2O$ and sodium ethoxide were mixed in ethanol solution and stirred at 70 °C for 3 h, which resulted in the formation of ruthenium ethoxide and sodium chloride, i.e.,

$$RuCl_3 + 3\,Na(OC_2H_5) \rightarrow Ru(OC_2H_5)_3 + 3\,NaCl \quad (1)$$

After 3 h, the solution was cooled and filtered to remove the precipitated sodium chloride and to obtain the ruthenium ethoxide solution. This ruthenium ethoxide solution was coated on a Pt (1 cm × 1 cm) working electrode and annealed in an oven at 180 °C for 2 h in air to produce the desired amorphous $RuO_2{\cdot}xH_2O$ active material. For preparation of the VGCF/$RuO_2{\cdot}xH_2O$ composite, a weighed quantity of VGCF was added to the ruthenium ethoxide solution, stirred for 24 h, cast on a Pt (1 cm × 1 cm) electrode, and finally annealed at 180 °C for 2 h. The ratio of the VGCF and $RuO_2{\cdot}xH_2O$ in the composite was estimated from the ratio of the VGCF and Ru precursors used in the synthesis. Since the as-synthesized material underwent partial dehydration of structural water during the synthesis, no attempt was made to calculate the hydration number (x) of the resultant $RuO_2{\cdot}xH_2O$ and hence, throughout this study, the weight of Ru metal has been used for calculating the loading of $RuO_2{\cdot}xH_2O$ in the VGCF/$RuO_2{\cdot}xH_2O$ nanocomposite.

The electrochemical characteristics and specific capacitance of the electrode materials were evaluated through cyclic voltammetric experiments (EG&G, model 273A) using a Ag/AgCl (3 M KCl, 0.196 V versus SCE, Metrohm) reference electrode and a Pt foil (2 cm × 2 cm) counter electrode. A Luggin capillary, whose tip was kept as close as 1 or 2 mm to the working electrode, was set to minimize the errors due to iR drop in the electrolyte. For all electrochemical characterizations, a test solution of 1.0 M H_2SO_4 was used as an electrolyte solution. The electrolyte solutions were purged with pure nitrogen for at least 30 min before use. In long-term cycle-life tests, the electrolyte solution was covered with a nitrogen blanket. Measurements of ac impedance (Autolab/FRA) were made with a three-electrode cell assembly at various bias potentials in the frequency range of 100 kHz to 0.01 Hz and with an ac perturbation of 5 mV. All the experiments were performed at room temperature. The loadings of active materials that were cast

on the Pt electrodes were determined with a digital weighing balance (Metler Toledo) that had a sensitivity of 1.0 μg. Analytical techniques such as X-ray diffraction spectroscopy (XRD) (Rigaku, D/MAX 2500H), thermo-gravimetric analysis (TGA) (TA instruments, 2940TMA) and scanning electron microscopy (SEM) (JEOL, JSM-6300) were used to analyze the chemical and structural nature of the active materials.

3. Results and discussion

The electrochemical performance of $RuO_2{\cdot}xH_2O$ is found to be greatly dependent on the method used for preparation, e.g., sol–gel process, electro-deposition, thermal decomposition of ruthenium ethoxide [14,17,19,20,35]. In the present study, thermal decomposition of ruthenium oxide has been chosen for the preparation of $RuO_2{\cdot}xH_2O$ and its composite with VGCF. This method allows the easy fabrication of electrode materials on the current-collector and, especially, avoids the usage of any non-conductive binder, so that better performance of the electrode materials are expected. Active materials of $RuO_2{\cdot}xH_2O$ and VGCF/$RuO_2{\cdot}xH_2O$ nanocomposite were obtained by following the experimental conditions as described in an earlier section. Since the process was conducted at 180 °C, the materials obtained were in the hydrous form of RuO_2, as this temperature is well below that for the crystallization of RuO_2 (>300 °C). The amorphous form of RuO_2 was confirmed by XRD analysis. The weight loss of the active materials between 180 and 300 °C was determined by TGA analysis. The values correspond to the structural water content in the as-synthesized RuO_2 and confirmed the hydrous nature of the as-prepared RuO_2. After the synthesis of the materials by heating at 180 °C for 2 h, the electrode materials were not subjected to further annealing, but were directly used for performance evaluation.

Scanning electrons micrographs of the pristine $RuO_2{\cdot}xH_2O$ and VGCF/$RuO_2{\cdot}xH_2O$ nanocomposite are shown in Fig. 1. The pristine $RuO_2{\cdot}xH_2O$ is composed primarily of small granular particles that are coated uniformly (thickness of coating: 250–300 nm) and densely on the current-collector. In the case of the VGCF/$RuO_2{\cdot}xH_2O$ nanocomposite, the $RuO_2{\cdot}xH_2O$ is found to deposit uniformly on the surface of the VGCF and the composite displays a well-dispersed and highly open structure. Such morphology is highly desirable for an electrode material to be used in supercapacitors. From the thickness of the composite fibre (∼800 nm), the thickness of $RuO_2{\cdot}xH_2O$ coating may be calculated as ∼325 nm, since that of pristine VGCF is ∼150 nm.

The electrochemical characteristics of these materials were studied through cyclic voltammetry using 1.0 M H_2SO_4 as an electrolyte, in the voltage range of 0–1.0 V at various potential scan rates. The results are presented in Fig. 2. In comparison with the pristine $RuO_2{\cdot}xH_2O$, the redox transitions of composite electrode are excellent, even at a very high scan rate of 1000 mV s^{-1} (Fig. 2(d)). Here, it should be mentioned that the loading of $RuO_2{\cdot}xH_2O$ in the composite is 33 wt.% of Ru. The redox transition curves of pristine $RuO_2{\cdot}xH_2O$ are far from ideal for a capacitor electrode at any one given scan rate, whereas the composite material shows perfect pseudocapacitive rectangular-like curves at every scan rate. Despite the small quantity of

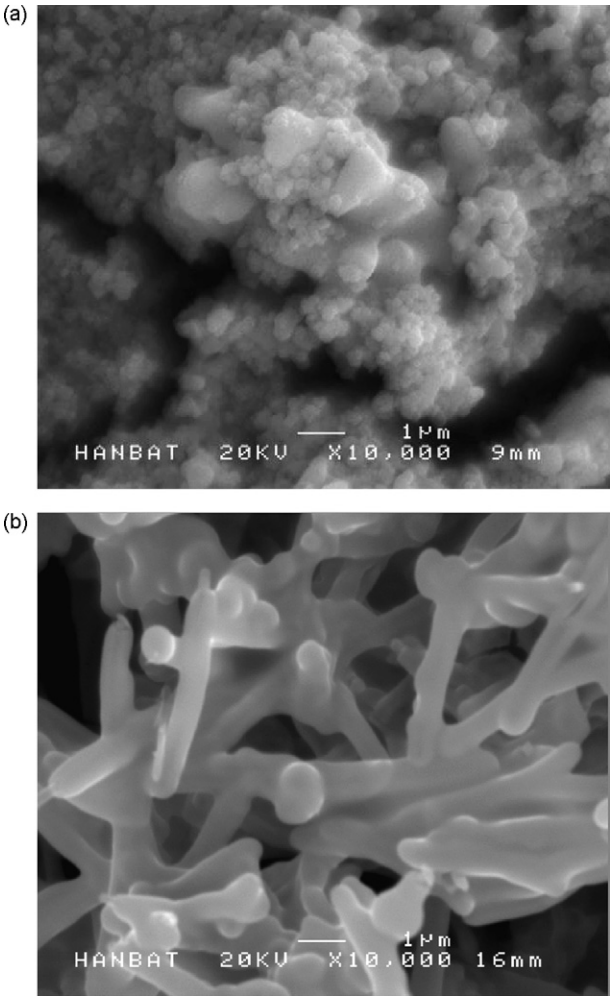

Fig. 1. Scanning electron micrographs of: (a) pristine $RuO_2{\cdot}xH_2O$ and (b) VGCF/$RuO_2{\cdot}xH_2O$ nanocomposite electrode materials.

$RuO_2{\cdot}xH_2O$ in the composite (33 wt.% of Ru), its current values are at least double those of pristine $RuO_2{\cdot}xH_2O$. From a control experiment, the specific capacitance of pristine VGCF is estimated to be only 1.9 F g^{-1}. Hence, the redox transition and the current values observed for the composite material should stem mainly from the Faradaic redox transitions of $RuO_2{\cdot}xH_2O$ in the composite. The specific capacitance values calculated from these CV curves are plotted in Fig. 3. At the lowest studied scan rate of 10 mV s^{-1}, the specific capacitances of pristine $RuO_2{\cdot}xH_2O$ and its composite are 410 and 1017 F g^{-1}, respectively, and at the highest scan rate of 1000 mV s^{-1}, the capacitance values are 258 and 824 F g^{-1}, respectively. So, the composite material is observed to show two-to-three times higher specific capacitance (based on Ru weight) than the pristine form of $RuO_2{\cdot}xH_2O$. Based on the total weight of the composite, however, its specific capacitance is more or less equal to that of pristine $RuO_2{\cdot}xH_2O$. Two important conclusions can be drawn from these results. First, even 33 wt.% of Ru in the composite stores a charge equal to that of 100 wt.% pristine $RuO_2{\cdot}xH_2O$. This demonstrates the effective utilization of $RuO_2{\cdot}xH_2O$ in the composite that is made possible through its better dispersion on the surface of VGCF. Second, at any given scan rate, and in comparison with pristine

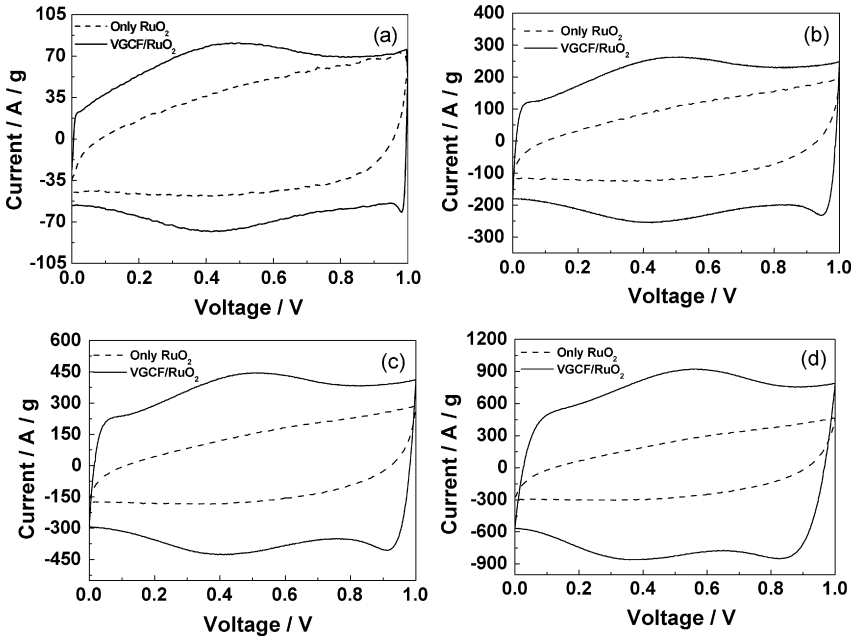

Fig. 2. Cyclic voltammograms of pristine $RuO_2{\cdot}xH_2O$ and VGCF/$RuO_2{\cdot}xH_2O$ nanocomposite electrodes recorded in 1.0 M H_2SO_4 at a scan rate of: (a) 100, (b) 300, (c) 500 and (d) 1000 mV s^{-1}.

$RuO_2{\cdot}xH_2O$, the redox transitions of the composite are excellent and the CV curves are perfectly pseudocapacitive. This difference is believed to be mainly due to VGCF offering good electronically conducting pathways to the $RuO_2{\cdot}xH_2O$ coated on its surface.

The capacitances of the present electrodes higher than those reported in certain studies [17,20,28,29,32–35,39,43–45] but lower than in other investigations [31,36–38,41,42,46]. These differences are caused mainly by differences in synthetic procedure, thickness/loading of $RuO_2{\cdot}xH_2O$, hydration number of $RuO_2{\cdot}xH_2O$, type of carbon matrix material used and its specific resistance and specific surface-area, etc. Nevertheless, the most important difference that we would like to stress is the excellent high-rate capability of the present VGCF/$RuO_2{\cdot}xH_2O$ nanocomposite material, which is better than that found in several of the published studies [32,41–43,47]. At 1000 mV s^{-1}, the capacitance retention of VGCF/$RuO_2{\cdot}xH_2O$ nanocomposite material is 81%, in comparison with that at 10 mV s^{-1}. Such a high-rate performance for RuO_2-based materials is very rare to observe in literature with the exception of $RuO_2{\cdot}xH_2O$ nanocrystallites prepared by a hydrothermal synthesis [48,49] and single crystalline RuO_2 nanorods formed by a chemical vapour deposition technique [50]. Very recently, Hu et. al. [47] have reported that the nanotubular $RuO_2{\cdot}xH_2O$ synthesized by a template-assisted method gave a capacitance retention of 60% at 1000 mV s^{-1} in comparison with that at 10 mV s^{-1} and was described as the best high-rate performance electrode that ever had been observed for $RuO_2{\cdot}xH_2O$ materials. Hence, present results of 81% capacitance retention at 1000 mV s^{-1} for the VGCF/$RuO_2{\cdot}xH_2O$ nanocomposite material outperforms the former report and demonstrates its ultrahigh power characteristics. It should also be noted that the thickness of the $RuO_2{\cdot}xH_2O$ coating over the VGCF is around 325 nm, which is also a fairly thick film unlike the high-rate performance claimed for very thin films (<10 nm thickness) in some studies [41,42]. This indicates the viability of the present VGCF/$RuO_2{\cdot}xH_2O$ nanocomposite electrodes to be used in practical cells. Due to the highly open structure of the VGCF/$RuO_2{\cdot}xH_2O$ nanocomposite electrodes, effective access of the electrolyte solution is favoured. Moreover, by combining the attributes of a homogeneous coating of the active $RuO_2{\cdot}xH_2O$ material on the VGCF surface and the very high electronically conducting support of VGCF offered to $RuO_2{\cdot}xH_2O$ paves the way for simultaneous efficient protonic and electronic transportation through the $RuO_2{\cdot}xH_2O$ material. This results in the fairly good specific capacitance and excellent high-rate performance of the composite material. The lower specific capacitance of the VGCF/$RuO_2{\cdot}xH_2O$ nanocomposite in comparison with some of the literature reports is understandable based on the lower specific surface-area of VGCF (13 m^2 g^{-1}) in comparison with the higher specific surface-area

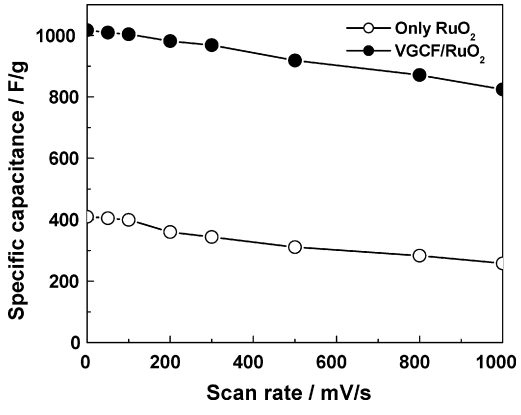

Fig. 3. Specific capacitance of pristine $RuO_2{\cdot}xH_2O$ and VGCF/$RuO_2{\cdot}xH_2O$ nanocomposite electrodes as function of scan rate.

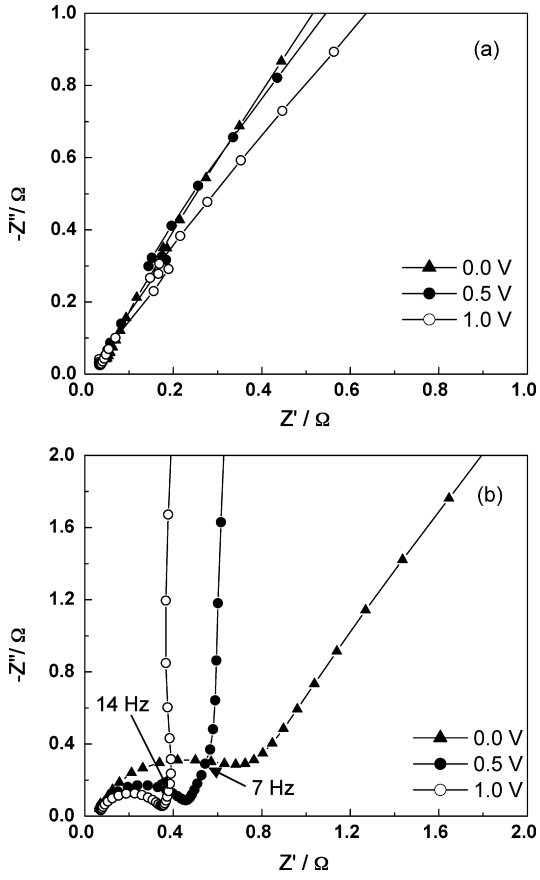

Fig. 4. Nyquist plots of: (a) pristine $RuO_2{\cdot}xH_2O$ and (b) VGCF/$RuO_2{\cdot}xH_2O$ nanocomposite electrodes measured at various bias potentials with ac frequency ranging from 100 kHz to 0.01 Hz.

(~2000 $m^2\,g^{-1}$) of activated carbon, CNT etc. used in those studies. There is, however, scope to improve the specific capacitance of the present composite material once high specific surface-area VGCF is used. Nonetheless, by virtue of its highly conducting nature of VGCF has definitely proved its scope as the best matrix that can be used for the dispersion of $RuO_2{\cdot}xH_2O$ to achieve high-rate performance from the electrode material.

To understand more about the electrochemical behaviour of $RuO_2{\cdot}xH_2O$ and its composite electrodes, ac impedance measurements were made on the electrodes at various applied bias potentials in a three-electrode cell configuration by applying frequency in the range of 100 kHz–0.01 Hz with an ac perturbation of 5 mV. The corresponding impedance spectra are given in Fig. 4. At all the bias potentials, pristine $RuO_2{\cdot}xH_2O$ electrodes show only a 45° inclined line of Warburg impedance, which indicates the dominance of diffusion-controlled resistance in the film. This is in quite good agreement with its CV results in that even at a low scan rate of 10 mV s^{-1}, the redox transitions are not purely capacitive-like during charging and discharging. This is possibly due to the compact morphology making a long, strained pathway for the diffusion of solvated ions into the $RuO_2{\cdot}xH_2O$ solid matrix, thus resulting in much of active materials being electrochemically inaccessible within the timeframe of CV (at 10 mV s^{-1}) and impedance (100 KHz to 0.01 Hz) measurements. On the other hand, the spectra of the VGCF/$RuO_2{\cdot}xH_2O$ composite are quite interesting and showed marked differences behaviour with respect to the change of bias potential. At all applied potentials, the electrodes display high-frequency semicircles, which are indicative of a charge-transfer resistance in parallel with a capacitive element. The diameter of the circles decreases markedly with increase in positive potential. On the face of it, a high-frequency, semi-circle corresponding to charge-transfer resistance for the composite electrodes is not expected as it is absent in the case of pristine $RuO_2{\cdot}xH_2O$. But, unlike the pristine $RuO_2{\cdot}xH_2O$ electrodes, so many interfaces exist in the composite electrodes, e.g., VGCF/VGCF, VGCF/$RuO_2{\cdot}xH_2O$, VGCF/$RuO_2{\cdot}xH_2O$/VGCF/$RuO_2{\cdot}xH_2O$. Thus, either in any one, or all, of these interfaces may impose some resistance to charge-transfer that thereby appears in impedance spectra [36]. This is also reasonable given that VGCF has a surface with a mixed hydrophilic and hydrophobic character and also a small aspect ratio (67). In fact, such evolution of a high-frequency semicircle has been often observed for carbon-based $RuO_2{\cdot}xH_2O$ composites [32,34,36,39,43]. However, when the bias potential is increased from 0 to 0.5 V, the VGCF/$RuO_2{\cdot}xH_2O$ composite electrode clearly exhibits a Warburg resistance in the mid-to-high frequency region and a perfect capacitive spike in the low-frequency region with a 'knee' frequency of 7 Hz. At the more positive potential of 1.0 V, the Warburg impedance is difficult to discern and the electrode displays capacitive domination from 14 Hz onwards. Such capacitive behaviour indicates that the diffusion of solvated ions in the composite material is not that difficult a process, as observed in the pristine $RuO_2{\cdot}xH_2O$ case, and the principal charge-storage process is not at all impeded by the small charge-transfer resistance that is observed in the high-frequency region. In addition, the magnitude of charge-transfer resistance is also not sufficiently high (0.3–0.8 Ω) to degrade the performance of the electrode.

Since long cycle-life is the most important criteria for a supercapacitor electrode, endurance tests for both types of electrode prepared in this study were undertaken by means of cycling the electrodes voltametrically between 0 and 1.0 V at a nominal scan rate of 300 mV s^{-1} for 10^4 times. The specific capacitance values calculated from the representative voltammograms

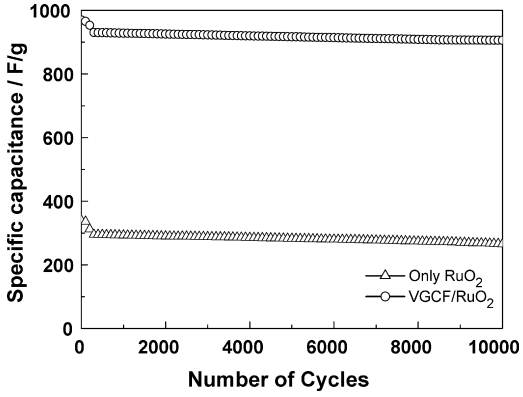

Fig. 5. Cycle-life of pristine $RuO_2{\cdot}xH_2O$ and VGCF/$RuO_2{\cdot}xH_2O$ nanocomposite electrodes obtained from voltammetric cycling between 0 and 1.0 V at a scan rate of 300 mV s^{-1}.

are plotted in Fig. 5. Both the electrodes give highly stable cycleability after about 300 cycles to until termination of the test, at which the capacitance retention of pristine $RuO_2{\cdot}xH_2O$ and VGCF/$RuO_2{\cdot}xH_2O$ nanocomposite electrodes 90 and 97%, respectively. Such extremely good cycleability is highly encouraging and warrants further development of these materials towards practical applications. The initial decline of capacitance during the 300 cycles is thought to be due to dissolution of a small amount of active materials. It may be noted that similar behaviour has been observed for CNT/$RuO_2{\cdot}xH_2O$ composite electrodes during continuous cycling [40].

By means of employing a higher specific surface-area VGCF (i.e., more than the present case), treating VGCF with acids to make it more hydrophilic, and optimizing both the loading of Ru over its surface and the annealing duration, further significant improvements in the specific capacitance values and the energy-power characteristics of the VGCF/$RuO_2{\cdot}xH_2O$ nanocomposite electrodes, may prove possible.

4. Conclusions

Electroactive materials of pristine $RuO_2{\cdot}xH_2O$ and VGCF/$RuO_2{\cdot}xH_2O$ nancomposite have been prepared by a thermal decomposition method. Pristine $RuO_2{\cdot}xH_2O$ is in the form of dense, granular particles, whereas, VGCF/$RuO_2{\cdot}xH_2O$ nanocomposite has a highly open and entangled structure. The VGCF fibres are coated uniformly with $RuO_2{\cdot}xH_2O$ to a thickness of ∼325 nm, which has a loading of 33 wt.% Ru. Cyclic voltammograms of pristine $RuO_2{\cdot}xH_2O$ are far deviated from those for an ideal capacitor, whereas the composite materials exhibit perfect rectangular-shaped capacitive curves. At the lowest studied scan rate of $10\,mV\,s^{-1}$, the specific capacitances of pristine $RuO_2{\cdot}xH_2O$ and its composite are 410 and $1017\,F\,g^{-1}$, respectively. At the highest scan rate of $1000\,mV\,s^{-1}$, the corresponding capacitance values are 258 and $824\,F\,g^{-1}$. The VGCF/$RuO_2{\cdot}xH_2O$ nanocomposite gives excellent high-rate performance and its capacitance retention at $1000\,mV\,s^{-1}$ is 81% in comparison with that at $10\,mV\,s^{-1}$. This is the highest value reported to date for $RuO_2{\cdot}xH_2O$-based electrodes with a thickness of ∼325 nm. Such a high-rate performance is believed to be due to the highly open morphology of the composite material, and to the highly electronically conducting support that it provides so as to favour optimization of proton and electron transportation through the $RuO_2{\cdot}xH_2O$ solid matrix. Analysis of ac impedance spectra of the pristine $RuO_2{\cdot}xH_2O$ electrode reveals that the diffusion of solvated ions within the pristine $RuO_2{\cdot}xH_2O$ matrix is the rate-determining step in the charge–discharge process. Both the pristine $RuO_2{\cdot}xH_2O$ and its composite electrodes give excellent stability and the capacitance retention over 10^4 cycles, namely, 90 and 97%, respectively.

Acknowledgement

This work was supported by Ministry of Commerce, Industry and Energy, Korea (MOCIE, Korea).

References

[1] B.E. Conway, Electrochemical Supercapacitors–Scientific Fundamentals and Technological Applications, Kluwer Academic Publisher, Plenum Press, Dordrecht, New York, USA, 1999.
[2] Y. Kibi, T. Saito, M. Kurata, J. Tabuchi, A. Ochi, J. Power Sources 60 (1996) 219.
[3] A. Yoshida, S. Nonaka, I. Aoki, A. Nishino, J. Power Sources 60 (1996) 207.
[4] M. Nakamura, M. Nakanishi, K. Yamamoto, J. Power Sources 60 (1996) 225.
[5] T. Morimoto, K. Hiratsuka, Y. Sanada, K. Kurihara, J. Power Sources 60 (1996) 239.
[6] D. Qu, H. Shi, J. Power Sources 74 (1998) 99.
[7] I. Bispo-Fonseca, J. Aggar, C. Sarrazin, P. Simon, J.F. Fauvarque, J. Power Sources 79 (1999) 238.
[8] R. Ma, J. Liang, B. Wei, B. Zhang, C. Xu, D. Wu, Bull. Chem. Soc. Jpn. 72 (1999) 2563.
[9] T. Momma, X. Liu, T. Osaka, Y. Ushio, Y. Sawada, J. Power Sources 60 (1996) 249.
[10] M. Ishikama, M. Ishikawa, A. Sakamoto, M. Morita, Y. Matsuda, K. Ishida, J. Power Sources 60 (1996) 233.
[11] H. Nagawa, A. Shudo, K. Miura, J. Electrochem. Soc. 147 (2000) 38.
[12] R.W. Pekala, J. Mater. Sci. 24 (1989) 3221.
[13] S.T. Mayer, R.W. Pekala, J.L. Kaschmitter, J. Electrochem. Soc. 140 (1993) 446.
[14] J.P. Zheng, P.J. Cygan, T.R. Jow, J. Electrochem. Soc. 142 (1995) 2699.
[15] J.W. Long, K.E. Swider, C.I. Merzbacher, D.R. Rolison, Langmuir 15 (1999) 780.
[16] D.A. McKeown, P.L. Hagans, L.P.L. Carette, A.E. Russell, K.E. Swider, D.R. Rolison, J. Phys. Chem. B 103 (1999) 4825.
[17] C.-C. Hu, Y.-H. Huang, Electrochim. Acta 46 (2001) 3431.
[18] W. Sugimoto, T. Kizaki, K. Yokoshima, Y. Murakami, Y. Takasu, Electrochim. Acta 49 (2004) 313.
[19] C.-C. Hu, W.-C. Chen, K.-H. Chang, J. Electrochem. Soc. 151 (2004) A281.
[20] J. Wen, Z. Zhou, Mater. Chem. Phys. 98 (2006) 442.
[21] W.-C. Fang, J.-H. Huang, L.-C. Chen, Y.-L.O. Su, K.-H. Chen, J. Power Sources 160 (2006) 1506.
[22] W. Sugimoto, K. Yokoshima, Y. Murakami, Y. Takasu, Electrochim. Acta 52 (2006) 1742.
[23] M. Toupin, T. Brousse, D. Belanger, Chem. Mater. 16 (2004) 3184.
[24] H. Kim, B.N. Popov, J. Electrochem. Soc. 150 (2003) D56.
[25] H.Y. Lee, J.B. Goodenough, J. Solid State Chem. 144 (1999) 220.
[26] K. Kinoshita, Carbon: Electrochemical and Physicochemical Properties, Wiley, New York, 1998.
[27] C.-C. Hu, Y.H. Huang, K.H. Chang, J. Power Sources 108 (2002) 117.
[28] M. Ramani, B.S. Haran, R.E. White, B.N. Popov, L. Arsov, J. Power Sources 93 (2001) 209.
[29] J. Zhang, D. Jiang, B. Chen, J. Zhu, L. Jiang, H. Fang, J. Electrochem. Soc. 148 (2001) A1362.
[30] C.-C. Hu, C.-C. Wang, Electrochem. Commun. 4 (2002) 554.
[31] H. Kim, B.N. Popov, J. Power Sources 104 (2002) 52.
[32] J.H. Jang, S. Han, T. Hyeon, S.M. Oh, J. Power Sources 123 (2003) 79.
[33] V. Panic, T. Vidakovic, S. Gojkovic, A. Dekanski, S. Milonjic, B. Nikolic, Electrochim. Acta 48 (2003) 3805.
[34] G. Arabale, D. Wagh, M. Kulkarni, I.S. Mulla, S.P. Vernekar, K. Vijayamohanan, A.M. Rao, Chem. Phys. Lett. 376 (2003) 207.
[35] J.H. Park, J.M. Ko, O.O. Park, J. Electrochem. Soc. 150 (2003)A864.
[36] C.-C. Hu, W.-C. Chen, Electrochim. Acta 49 (2004) 3469.
[37] C.-C. Wang, C.-C. Hu, Mater. Chem. Phys. 83 (2004) 289.
[38] W.-C. Chen, C.-C. Hu, C.-C. Wang, C.-K. Min, J. Power Sources 125 (2004) 292.
[39] M.S. Dandekar, G. Arabale, K. Vijayamohanan, J. Power Sources 141 (2005) 198.
[40] J.-S. Ye, H.F. Cui, X. Liu, T.M. Lim, W.-D. Zhang, F.-S. Sheu, Small 1 (2005) 560.

[41] I.-H. Kim, J.-H. Kim, K.-B. Kim, Electrochem. Solid-State Lett. 8 (2005) A369.
[42] I.-H. Kim, J.-H. Kim, Y.-H. Lee, K.-B. Kim, J. Electrochem. Soc. 152 (2005) A2170.
[43] M. Min, K. Machida, J.H. Jang, K. Naoi, J. Electrochem. Soc. 153 (2006) A334.
[44] G.-Y. Yu, W.-X. Chen, Y.-F. Zheng, J. Zhao, X. Li, Z.-D. Xu, Mater. Lett. 60 (2006) 2453.
[45] I.-H. Kim, K.-B. Kim, J. Electrochem. Soc. 153 (2006) A383.
[46] J.-K. Lee, H.M. Pathan, K.-D. Jung, O.-S. Joo, J. Power Sources 159 (2006) 1527.
[47] C.-C. Hu, K.-H. Chang, M.-C. Lin, Y.-T. Wu, Nano Lett 6 (2006) 2690.
[48] K.H. Chang, C.-C. Hu, Electrochem. Solid-State Lett. 7 (2004) A466.
[49] K.H. Chang, C.-C. Hu, Appl. Phys. Lett. 88 (2006) 193102.
[50] Y.F. Ke, D.S. Tsai, Y.S. Huang, J. Mater. Chem. 15 (2005) 2122.